Neuron, Vol. 43, 333–344, August 5, 2004, Copyright ©2004 by Cell Press

LRP/Amyloid β-Peptide Interaction Mediates Differential Brain Efflux of Aβ Isoforms

Rashid Deane,[1,5] Zhenhua Wu,[1,5] Abhay Sagare,[1] Judianne Davis,[2] Shi Du Yan,[3] Katie Hamm,[1] Feng Xu,[2] Margaret Parisi,[1] Barbra LaRue,[1] Hong Wei Hu,[3] Patricia Spijkers,[4] Huang Guo,[1] Xiaomei Song,[1] Peter J. Lenting,[4] William E. Van Nostrand,[2] and Berislav V. Zlokovic[1,*]

[1]Frank P. Smith Laboratories for Neuroscience and Neurosurgical Research
Department of Neurosurgery
Division of Neurovascular Biology
Arthur Kornberg Medical Research Building
University of Rochester Medical Center
Rochester, New York 14642
[2]Department of Medicine
Health Sciences Center
Stony Brook University
Stony Brook, New York 11794
[3]Department of Pathology
Department of Surgery
College of Physicians and Surgeons of Columbia University
New York, New York 10032
[4]Laboratory for Thrombosis and Haemostasis
Department of Hematology
University Medical Center Utrecht
3584 CX Utrecht
The Netherlands

Summary

LRP (low-density lipoprotein receptor-related protein) is linked to Alzheimer's disease (AD). Here, we report amyloid β-peptide Aβ40 binds to immobilized LRP clusters II and IV with high affinity (K_d = 0.6–1.2 nM) compared to Aβ42 and mutant Aβ, and LRP-mediated Aβ brain capillary binding, endocytosis, and transcytosis across the mouse blood-brain barrier are substantially reduced by the high β sheet content in Aβ and deletion of the receptor-associated protein gene. Despite low Aβ production in the brain, transgenic mice expressing low LRP-clearance mutant Aβ develop robust Aβ cerebral accumulations much earlier than Tg-2576 Aβ-overproducing mice. While Aβ does not affect LRP internalization and synthesis, it promotes proteasome-dependent LRP degradation in endothelium at concentrations >1 μM, consistent with reduced brain capillary LRP levels in Aβ-accumulating transgenic mice, AD, and patients with cerebrovascular β-amyloidosis. Thus, low-affinity LRP/Aβ interaction and/or Aβ-induced LRP loss at the BBB mediate brain accumulation of neurotoxic Aβ.

Introduction

The low-density lipoprotein receptor-related protein (LRP), a member of the low-density lipoprotein receptor (LDLR) family, is a multiligand receptor whose physiological functions are carried out by endocytosis of ligands and activation of multiple signal transduction pathways (Herz and Strickland, 2001; Herz and Marschang, 2003). The precursor form of LRP, a 600 kDa transmembrane glycoprotein, is cleaved in *trans*-Golgi network by furin to generate 515 kDa α subunit and 85 kDa β subunit that remain noncovalently associated during LRP transport to the cell membrane (Herz et al., 1990). A 39 kDa receptor-associated protein (RAP) is a specialized chaperone molecule that binds to LRP and regulates its proper folding (Bu, 2001). LRP interacts with a broad range of secreted proteins and resident cell surface molecules in the brain (>30 structurally diverse ligands), mediating their endocytosis and/or activating signaling pathways through multiple cytosolic adaptor and scaffold proteins (Herz, 2001). Phosphorylation of LRP's tail regulates ligand internalization and signal transduction (van der Geer, 2002; Green and Bu, 2002).

LRP is linked to Alzheimer's disease (AD) by genetic and biochemical evidence. Genetic polymorphism in *LRP* gene is associated with late-onset AD (Kang et al., 1997; Hollenbach et al., 1998; Lambert et al., 1998; Wavrant-DeVrieze et al., 1999). In addition, LRP binds amyloid β-peptide (Aβ) precursor protein (APP), apolipoprotein E (apoE), and α_2-macroglobulin (α_2M), which have been genetically linked to AD (Herz and Strickland, 2001). The exact pathogenic mechanism(s) by which LRP contributes to neurotoxic Aβ accumulations is unclear. LRP binds secreted APP and influences its degradation (Kounnas et al., 1995) and processing (Pietrzik et al., 2002), leading to increased Aβ production (Ulery et al., 2000). It may be involved in α_2M-mediated slow reuptake of secreted Aβ by neurons derived from transgenic APP mice and in mouse fibroblasts with no degradation of Aβ (Qiu et al., 1999; Kang et al., 2000). Slow degradation of Aβ via α_2M in mouse fibroblasts and U97 human glioma cells has also been suggested (Narita et al., 1997). ApoE3 may prevent Aβ neurotoxicity by forming complexes with Aβ, and its protective effect possibly requires LRP (Jordán et al., 1998), although the role of other lipoprotein receptors, e.g., LDLR and megalin, cannot be ruled out.

However, overexpression of functional LRP minireceptors in neurons of Alzheimer's PDAPP mice results in age-dependent increases of soluble Aβ in the brain (Zerbinatti et al., 2004), suggesting LRP on neurons in vivo does not mediate Aβ clearance.

LRP is expressed in brain capillary endothelium (Shibata et al., 2000; Wang et al., 2003). The idea that LRP along the brain capillary membranes clears Aβ in vivo has been supported by brain efflux studies with exogenous soluble Aβ40, suggesting that the blood-brain barrier (BBB) is a primary clearance site for Aβ (Shibata et al., 2000). However, neither this nor other studies have clarified at the molecular and cellular level how LRP at the BBB works as a cargo/clearance receptor for Aβ and whether LRP on brain capillaries clears neurotoxic Aβ42 (Hardy and Selkoe, 2002) and vasculotropic Aβ mutants (Vinters and Farag, 2003). Reduced levels of

*Correspondence: berislav_zlokovic@urmc.rochester.edu
[5]These authors contributed equally to this work.

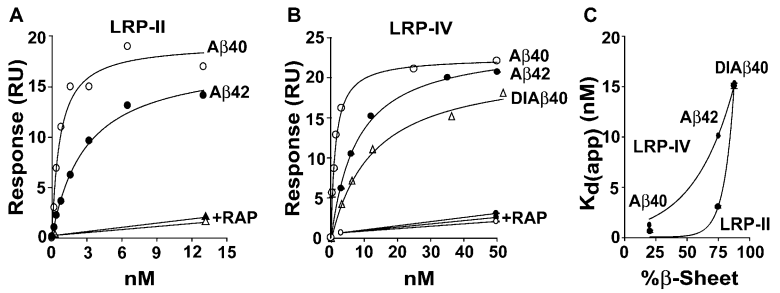

Figure 1. SPR Analysis of the Interaction between Aβ and Recombinant LRP Fragments

(A) Differential binding of Aβ40 and Aβ42 to LRP cluster II immobilized at a CM5 chip at a density of 10 fmol/mm^2. Incubation conditions as in Experimental Procedures.

(B) Differential binding of Aβ40, Aβ42, and mutant Aβ (Dutch/Iowa40, DIAβ40) to immobilized LRP cluster IV under conditions as in (A).

(C) Kinetic parameters for the binding of different Aβ species to LRP plotted against the content of β sheets in Aβ peptides determined by circular dichroism analysis. Apparent affinity constants $K_{d(app)}$ were deferred from the ratios of $k_{off(app)}/k_{on(app)}$ as described in Experimental Procedures. Means ± SEM (n = 3–5); SEM ≤ 5% of the mean in (A) and (B). $K_{d(app)}$ (mean ± SD) values were determined from 6–9 different concentrations of Aβ and 3–5 independent measurements at each concentration. RAP, receptor-associated protein (500 nM); RU, resonance units.

LRP in AD have been associated with Aβ brain accumulations (Kang et al., 1997, 2000; Shibata et al., 2000), but whether Aβ directly interferes with LRP's internalization, degradation, and/or synthesis at the clearance site(s) in brain is not known.

Here, we provide evidence for a direct LRP/Aβ protein-protein interaction and demonstrate that this interaction on brain capillaries regulates in an isoform-specific manner binding of Aβ to LRP followed by Aβ endocytosis and transcytosis across the BBB. We report that LRP at the BBB favors clearance of Aβ40 relative to a high β sheet content Aβ42 and vasculotropic mutant Aβ, while deletion of the RAP gene/depletion of LRP (Veinbergs et al., 2001), but not of the LDLR and VLDLR genes, precludes rapid Aβ brain capillary clearance and efflux at the BBB. Transgenic mice producing low LRP-clearance mutant Aβ in the brain develop robust Aβ accumulations compared to Tg-2576 wild-type Aβ-overproducing mice (Hsiao et al., 1996), despite >20-fold lower brain APP expression and >30-fold reduced Aβ neuronal production. Finally, we show Aβ does not affect LRP internalization or synthesis but promotes proteasome-dependent LRP degradation at pathological levels consistent with low LRP activity in brain microvessels in Aβ-accumulating mice and in patients with AD and familial cerebrovascular β-amyloidosis.

Results

Figures 1A and 1B show high-affinity binding of monomeric Aβ40 to immobilized LRP clusters II and IV with K_d values of 0.57 ± 012 and 1.24 ± 0.01 nM, respectively, determined by the surface plasmon resonance (SPR) analysis. In contrast, Aβ42 and vasculotropic mutant Aβ (Dutch/Iowa Aβ40 double mutant model peptide; Van Nostrand et al., 2001) exhibit greatly reduced binding affinity for LRP clusters II and IV by 6- and 9-fold and 28- and 12-fold, respectively, compared to Aβ40. The K_d values for Aβ42 binding to LRP II and IV clusters were 3.00 ± 0.11 and 10.10 ± 0.03 nM, respectively, and for mutant Aβ, 15.10 ± 0.10 and 15.30 ± 0.07 nM, respectively. Binding of Aβ to LRP was abolished by RAP, an LRP antagonist (Figures 1A and 1B; Herz and Strickland, 2001). Its affinity to immobilized LRP fragments was greatly reduced by the high content of β sheets (Figure 1C).

Figure 2A shows differential LRP-dependent binding of Aβ isoforms at the abluminal side of brain capillaries, i.e., Aβ40 > Aβ42 > Dutch/Iowa Aβ40, and no binding of the reverse 40-1 peptide, consistent with the SPR findings (Figure 1). Binding of Aβ was displaced by RAP and LRP-specific IgG (Figure 2A) and excess of unlabeled ligand (not shown). Figure 2B illustrates differential LRP-mediated internalization of ^{125}I-labeled Aβ isoforms into brain endothelium, i.e., Aβ40 > Aβ42 > DIAβ40, and inhibition (>85%) with RAP and LRP-specific IgG. The half-time ($t_{1/2}$) of LRP internalization in the presence of different Aβ isoforms was similar between 26 and 30 s (Figure 1C). During internalization, there was no significant degradation of Aβ by brain endothelium as indicated by negligible non-trichloracetic acid (TCA)-precipitable counts in brain capillary cell lysates (Figure 1D) and in the medium (not shown). The short-term kinetic uptake studies at 37°C confirmed a saturable LRP-dependent clearance of Aβ40 by brain capillaries with the Michaelis constant K_m of 10 ± 2 nM and >85% inhibition of uptake by RAP and LRP-specific IgG (Figure 2D). The kinetic inhibitory constants, K_i, confirmed that Dutch Aβ40, wild-type Aβ42, Dutch Aβ42, and Dutch/Iowa Aβ40 exhibit 6-, 14-, 18-, and 22-fold lower affinities for LRP-mediated brain capillary clearance than Aβ40, respectively (Figure 2E).

Next, we compared [^{125}I]Aβ clearance by brain microvessels derived from RAP null, LDLR null, VLDLR null, and control mice. The Western blot analysis indicated that LRP in brain capillaries of RAP null mice was decreased by >75% compared to controls (Figure 3A), while VLDLR and LDLR levels were reduced by approximately 40%. LRP-positive vascular profiles in different brain regions in RAP null mice were reduced to 14%–16% versus 60%–70% in controls, as indicated by double staining for LRP and endothelial cell marker CD31 (Figures 3B and 3C). Deletion of the RAP gene resulted in about 80% reduction in brain capillary clearance of Aβ40, Aβ42, and DIAβ40 (Figure 3D), while deletion of the VLDLR and LDLR genes did not significantly affect Aβ clearance (Figure 3E).

Figure 4A compares efflux across the BBB of ^{125}I-labeled Aβ40 and mutant Aβ (Dutch/Iowa Aβ40) microinfused simultaneously with [^{14}C]inulin (reference marker) into brain ISF, as described (Shibata et al., 2000). In vivo transcytosis rates of ^{125}I-labeled Aβ at the BBB were obtained after correcting for the tracer's passive diffu-

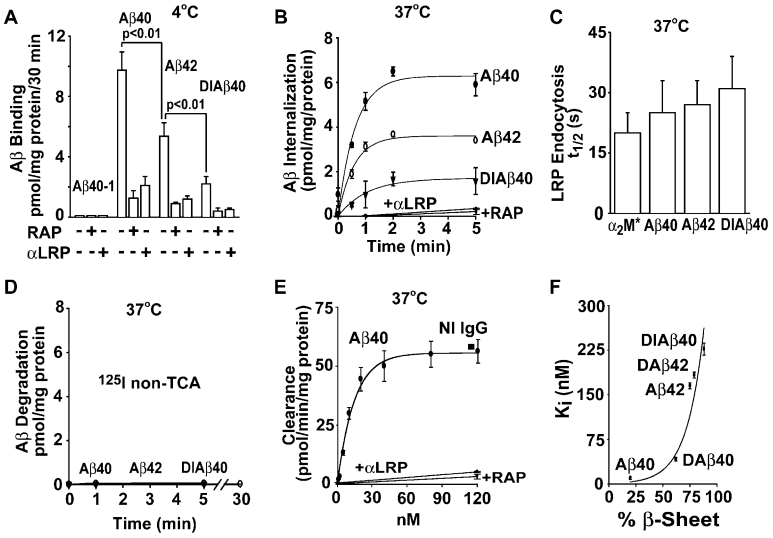

Figure 2. LRP-Mediated Aβ Binding, Internalization, and Clearance on Mouse Brain Capillaries

(A) Binding of [^{125}I]Aβ ligands (2 nM) to the abluminal brain capillary surface was determined at 4°C for 30 min. RAP (500 nM); αLRP, LRP-specific IgG (Fab_2, 60 μg/ml); Aβ40-1, reverse Aβ40 peptide.

(B) Internalization of Aβ peptides at the abluminal brain capillary surface. Capillaries were incubated with [^{125}I]Aβ ligands (2 nM) at 4°C for 30 min and than at 37°C for the indicated times. The fraction of internalized ligand was calculated as in the Experimental Procedures and plotted against the internalization time. RAP (500 nM); αLRP (60 μg/ml).

(C) The half-time ($t_{1/2}$) of LRP endocytosis determined with α_2M* and different Aβ ligands from (B).

(D) Undetectable ^{125}I non-TCA precipitable counts (^{125}I non-TCA) in lysed BEC during internalization of [^{125}I]Aβ ligands (2 nM).

(E) Rapid saturable Aβ40 uptake by brain capillaries determined at 37°C within 1 min using [^{125}I]Aβ40 (1 nM) and increasing concentrations of unlabeled Aβ (1–120 nM). RAP (1 μM); αLRP and a nonimmune IgG, NI IgG (60 μg/ml).

(F) K_i (inhibitory constant) for LRP-mediated brain capillary clearance of Aβ isoforms plotted against Aβ β sheet content. K_i values were determined with [^{125}I]Aβ40 (2 nM) and 40 nM unlabeled Aβ40, Aβ42, and mutant Aβ (Dutch40, DAβ40; Dutch42, DAβ42; Dutch/Iowa40, DIAβ40). Means ± SEM (n = 3–5).

sion via the ISF bulk flow by subtracting the elimination rate of [^{14}C]inulin, as explained in the Experimental Procedures. At concentrations comparable to physiological levels of soluble Aβ in brain ISF (i.e., ≤1 nM) (Cirrito et al., 2003), Aβ40 was cleared rapidly across the BBB within a few seconds. In contrast, only 40% of mutant Aβ was cleared across the BBB over a much longer time period of 30 min. At higher concentrations, mutant Aβ was almost devoid of clearance at the BBB, while Aβ40 still exhibited a substantial clearance. RAP and an anti-LRP antibody, but not a nonimmune immunoglobulin G (NI IgG) (Figure 4A), almost abolished Aβ elimination across the BBB.

A significant ($p < 0.05$) crossinhibition of [^{125}I]Aβ40 efflux at the BBB by unlabeled Aβ42 and mutant Aβ and a pronounced >95% inhibition of ^{125}I-labeled Aβ42 and mutant Aβ clearance by unlabeled wild-type Aβ40 (Figure 4B) indicated that all Aβ peptides compete for the same LRP-mediated efflux system to exit the brain, and Aβ40 exerts a significant retention effect on Aβ42 and mutant Aβ in vivo. All Aβ test ligands microinfused into brain ISF in the presence of unlabeled Aβ remained >97% in their monomeric forms (Shibata et al., 2000; Zlokovic et al., 2000), as confirmed by the HPLC (Figure 4B, insets) and SDS-PAGE analyses (not shown) of brain homogenates. During relatively short incubation time and low nM levels of [^{125}I]Aβ ligand and the cold peptide, [^{125}I]Aβ did not bind to unlabeled Aβ, consistent with reports suggesting significantly higher concentrations of Aβ, and longer times are required for Aβ oligomerization or aggregation (Dahlgren et al., 2002; Kayed et al., 2003).

The K_i values indicated that Aβ42 and mutant Aβ exhibit 8- and 15-fold lower affinity for LRP-mediated efflux at the BBB in vivo than Aβ40, consistent with their high β sheet content (Figure 4C). There was 75% to 85% inhibition of Aβ40 and Aβ42 rapid efflux across the BBB in RAP null/severely depleted LRP mice (Figure 4D), while deletion of the LDLR and VLDR genes did not significantly affect Aβ clearance at the BBB (Figure 4D). Since LDLR and VLDLR do not contribute to rapid Aβ clearance in RAP null mice (Figures 3E and 4D) and LRP on neurons in vivo does not mediate Aβ clearance (Zerbinatti et al., 2004), one can speculate that increased amount of amyloid in double crossed RAP null/APP overexpressing mice (Van Uden et al., 2002) could be related to inefficient LRP-mediated Aβ clearance across the BBB.

To validate our clearance hypothesis for endogenous Aβ, we compared Aβ accumulation in transgenic Dutch/Iowa (Tg-DI) mice expressing low levels of human APP under control of Thy 1.2 neuronal promoter harboring the Dutch (Levy et al., 1990) and Iowa (Grabowski et al., 2001) vasculotropic mutations (Davis et al., 2004) versus Tg-2576 APP overexpressing mice (Hsiao et al., 1996). Tg-DI mice produce mainly mutant Aβ40 (Dutch/Iowa) (Figure 5C) that, compared to the wild-type Aβ40, binds to LRP with significantly lower affinity (Figures 2B and 2C) and exhibits low LRP-clearance on brain capillaries (Figures 2B and 3D) and across the BBB (Figures 4A and 4C). At 3, 6, and 12 months of age, APP levels in the brain of Tg-DI mice versus Tg-2576 mice were considerably lower by 24-fold (Figures 5A and 5B, left). In fact, the Tg-DI mice express human APP at <50% the levels of endogenous mouse APP, as reported in three independent lines (Davis et al., 2004). Despite substantially lower levels of human APP (Figure 5B, left) and >30-fold lower neuronal production of Aβ compared to Tg-2576 mice (Figure 5B, right), the Tg-DI mice exhibited earlier onset and more robust brain accumulations of Aβ than Tg-2576 mice (Figure 5C), i.e., by 15- and 5-fold higher for the 40 and 42 isoforms, respectively, at 6 months of age.

Tg-DI mice developed early Aβ plaque-like deposits in the cortex and hippocampus at 3 months of age (Fig-

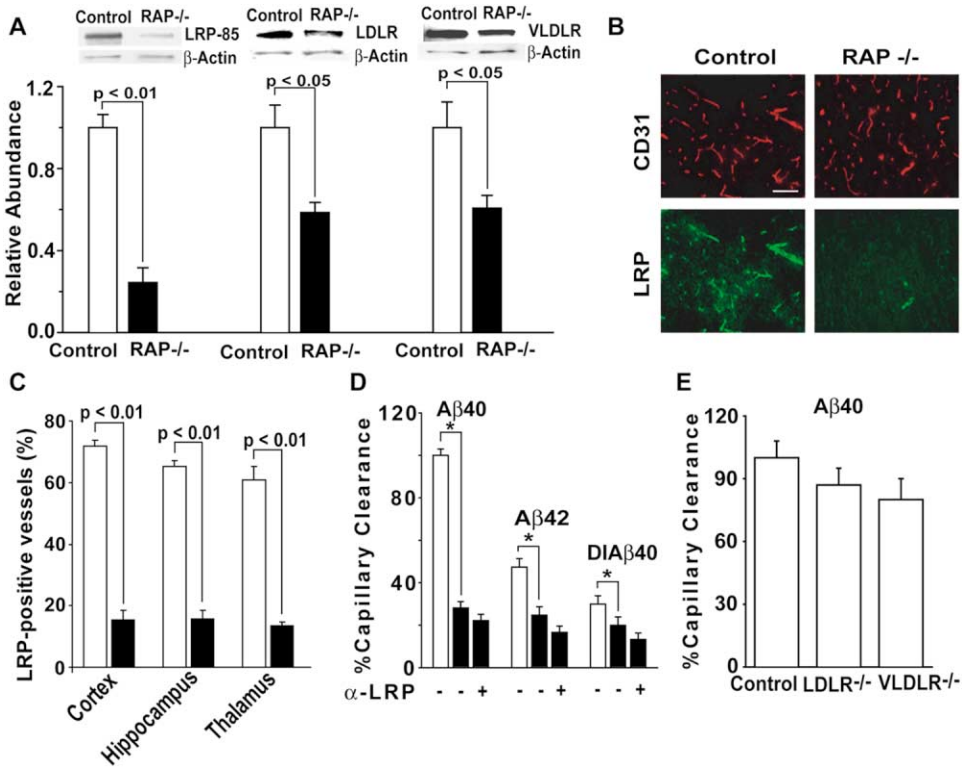

Figure 3. Low LRP-Mediated Aβ Clearance on Brain Microvessels in RAP Null Mice

(A) LRP, LDLR, and VLDLR brain capillary levels in wild-type and RAP null ($RAP^{-/-}$) mice by Western blot analysis. LRP-85, LRP β-chain-specific IgG (5A6). Scanning densitometry of LRP, LDLR, and VLDLR bands relative to β-actin in wild-type (control, open bar) and $RAP^{-/-}$ (closed bar) mice.

(B) Double immunostaining for LRP and CD31 (endothelial cell marker) in brain tissue sections in wild-type (control) and RAP null mice; scale bar equals 50 μm.

(C) LRP-positive vascular profiles in different brain regions in wild-type mice (open bars) and RAP null mice (closed bars).

(D) Brain capillary clearance of ^{125}I-labeled Aβ40, Aβ42, and mutant Aβ (Dutch/Iowa40, DIAβ40) in wild-type mice (open bars) and RAP null mice (closed bars) studied at 1 nM peptides concentration. *p $<$ 0.01 RAP null compared to controls; αLRP, LRP-specific N20 polyclonal antibody (60 μg/ml).

(E) Brain capillary clearance of [^{125}I]Aβ40 (1 nM) in LDLR null and VLDLR null mice. Means ± SEM (n = 3–5).

ure 5D, left), while the Tg-2576 mice (Hsiao et al., 1996; Kawarabayashi et al., 2001) initially present Aβ deposits at ~9 months of age (not shown). Similarly, the APP/PS-1 knockin mice homozygous for both the humanized APP and the PS-1 knockin mutation, which causes an increase in the amount of Aβ42, only develop Aβ deposits at ~6 months of age (Flood et al., 2002). Abundant Aβ plaque-like diffuse deposits with significant microvascular intracerebral association were found in Tg-DI mice at 12 months (Figure 5D, right). Plasma levels of mutant Aβ in Tg-DI mice were extremely low, i.e., <25 pM, consistent with the low clearance across the BBB (Figure 4A). Double immunostaining for LRP and endothelial cell marker CD31 indicated substantial reduction of LRP-positive vascular profiles in several brain regions in Tg-DI and Tg-2576 mice at 4–6 months of age, i.e., only 5%–20% and 25%–30% of microvessels were positive for LRP, respectively, compared to 65%–75% of LRP-positive vessels in age-matched littermate controls (Figure 5E). Significant LRP brain capillary reduction in transgenic mice was confirmed by Western blot analysis (Figure 5F). The decrease in LRP vascular profiles at 12 months of age was also more pronounced in Aβ-accumulating transgenic mice than in controls (Figure 5G).

Figures 6A–6D indicate that Aβ40, Aβ42, and/or mutant Aβ (Dutch/Iowa Aβ40) at lower concentrations (≤10 nM) do not alter LRP expression in primary human brain endothelial cells (BEC). However, at levels ≥1 μM over longer periods of time (i.e., 48 hr), all Aβ species downregulated LRP in BEC in a concentration-dependent manner, as demonstrated for LRP 85 kDa β subunit (Figures 6A–6D) and 515 kDa α subunit (not shown). RAP and LRP-specific IgG, but not a control nonimmune IgG (not shown), blocked Aβ-induced LRP downregulation. Aβ treatment did not reduce the expression of other cell surface receptors in BEC, as, for example, the levels of the receptor for advanced glycation end products (RAGE) were increased (not shown) as reported (Deane et al., 2003) and the levels of transferrin receptor remain unchanged (not shown). TUNEL and Hoechst staining in BEC were negative, and the levels of lactic acid dehydrogenase in the medium did not increase from control values (not shown).

Aβ40, Aβ42, and mutant Aβ at 20 μM over 48 hr significantly reduced (>60%) the amount of internalized [^{125}I]α2M* into human BEC (Figure 7A), consistent with significantly reduced LRP levels (Figure 6D). However, this treatment did not significantly alter the LRP endocy-

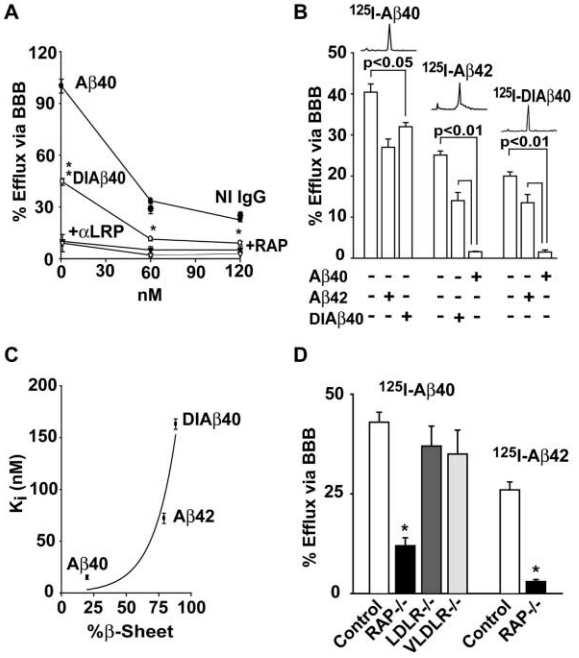

Figure 4. LRP-Mediated Transport of Aβ across the Mouse BBB In Vivo

(A) Efflux of mutant Aβ (Dutch/Iowa40, DIAβ40; open points) versus wild-type Aβ40 (solid points) across the BBB within 30 min of brain ISF [^{125}I]Aβ microinjections at 1–120 nM carrier concentration. RAP (1 μM); αLRP, LRP-specific IgG (60 μg/ml); NI IgG, nonimmune IgG (60 μg/ml; closed square). *$p < 0.05$ and **$p < 0.01$ for DIAβ40 versus Aβ40.

(B) Efflux across the BBB of ^{125}I-labeled Aβ40, Aβ42, and mutant Aβ (Dutch/Iowa40, DIAβ40) at 40 nM in the absence and presence of unlabeled Aβ (120 nM). [^{125}I]Aβ monomers (HPLC analysis) in brain homogenates 30 min after microinfusion of ^{125}I/unlabeled Aβ mixture into brain ISF (insets above bars).

(C) K_i values for LRP-mediated efflux at the BBB of Aβ40, Aβ42, and mutant Aβ (Dutch/Iowa40; DIAβ40) plotted against Aβ β sheet content. K_i values were determined with [^{125}I]Aβ40 at 40 nM and unlabeled Aβ at 120 nM.

(D) Aβ40 and Aβ42 efflux across the BBB in RAP null mice (RAP$^{-/-}$; closed bars) versus wild-type mice (control, open bars), and Aβ40 efflux in LDLR null and VLDLR null mice. Means ± SEM (n = 3–8).

tosis rate, and the $t_{1/2}$ for LRP endocytosis in the presence of different Aβ isoforms remained unchanged compared to controls, i.e., about 15 s (Figure 7B). On the other hand, the pulse-chase studies revealed that Aβ42 (20 μM) decreases the half-life ($t_{1/2}$) for LRP from 9.6 to 6.4 hr (Figures 7C and 7D). MG132, an inhibitor of the proteasome-dependent LRP degradation (Melman et al., 2002), increased the $t_{1/2}$ for LRP in control and Aβ-treated cells (Figures 7E and 7F). Immunoblot analysis with an anti-LRP C-terminal antibody that recognizes an immature 600 kDa form of LRP confirmed that the levels of immature LRP are not affected by Aβ treatment (Figure 7G), suggesting no effect on LRP synthesis.

LRP-positive vascular profiles in human brain tissue revealed greatly reduced LRP expression in patients with AD and cerebrovascular β-amyloidosis Dutch-type compared to age-matched controls (Figures 8A and 8B). The number of LRP-positive cerebral vessels dropped from 45% in age-matched controls to ~12% in AD and was barely detectable in patients with Dutch-type cerebrovascular β-amyloidosis.

Discussion

Aβ accumulation in the brain is a chief pathogenic event (Hardy and Selkoe, 2002). Increased Aβ42 levels lead to formation of neurotoxic Aβ oligomers, resulting in progressive synaptic, neuritic, and neuronal dysfunction (Walsh et al., 2002; Dahlgren et al., 2002; Kayed et al., 2003; Gong et al., 2003). Missense mutations inside the Aβ sequence associate with vascular deposits in patients with the Dutch mutation (G to C at codon 693, Glu to Gln at position 22; Levy et al., 1990) and Iowa mutation (G to A at codon 694, Asp to Asn at position 23; Grabowski et al., 2001). How Aβ accumulates in the brain is unclear. Increased Aβ production can explain a small fraction of early onset AD familial cases bearing inherited mutations in the APP gene flanking the Aβ coding region (i.e., Swedish mutation) or PS-1 or -2 genes. This leaves inefficient Aβ clearance as a major mechanism mediating Aβ cerebral accumulation in late-onset AD (Selkoe, 2001; Zlokovic and Frangione, 2003) and familial forms of cerebrovascular β-amyloidoses (Ghiso and Frangione, 2002).

Here, we report LRP/Aβ direct interaction at the BBB critically influences Aβ brain accumulation by promoting retention of high β sheet neurotoxic Aβ42 and vasculotropic mutant Aβ while clearing soluble Aβ40 from brain ISF to blood. The SPR analysis (Figure 1) used as a first step to characterize Aβ interaction with the LRP ligand binding domains (Herz and Strickland, 2001) revealed that Aβ40 binds to LRP with high affinity compared to Aβ42 and mutant Aβ. Consistent with the SPR findings, we next showed that LRP-mediated Aβ brain capillary binding and endocytosis in vitro and transcytosis across the BBB in vivo in mice are substantially reduced by the high β sheet content in Aβ (Figures 2–4) and deletion of the RAP gene, but not the LDLR and VLDLR genes (Figures 3–4).

In contrast to remarkable LRP-mediated Aβ40 binding and endocytosis at the abluminal side of brain microvessels (Figures 2 and 3) and abluminal to luminal transcytosis across the BBB in vivo (Figure 4), our earlier study failed to detect significant receptor-mediated Aβ40 basolateral to apical transport in cultured brain endothelial monolayers (Mackic et al., 1998). It is possible that the density of LRP receptors at the basolateral membrane in the monolayer cultures (Mackic et al., 1998) was much lower than at the abluminal membrane of freshly isolated brain capillaries and at the BBB in vivo (Figures 2–4), which could account for the loss of LRP-dependent Aβ40 basolateral to apical flux in monolayers (Mackic et al., 1998) and may explain the discrepancies between results obtained in the monolayer transport model versus present and previous study (Shibata et al., 2000).

The present data show that rapid interaction of Aβ with LRP does not require chaperone molecules. However, this does not rule out the possibility that Aβ may also interact with LRP via chaperone molecules. Thus, both direct and indirect interaction of Aβ with LRP may exist in parallel. For example, α_2M can mediate via LRP

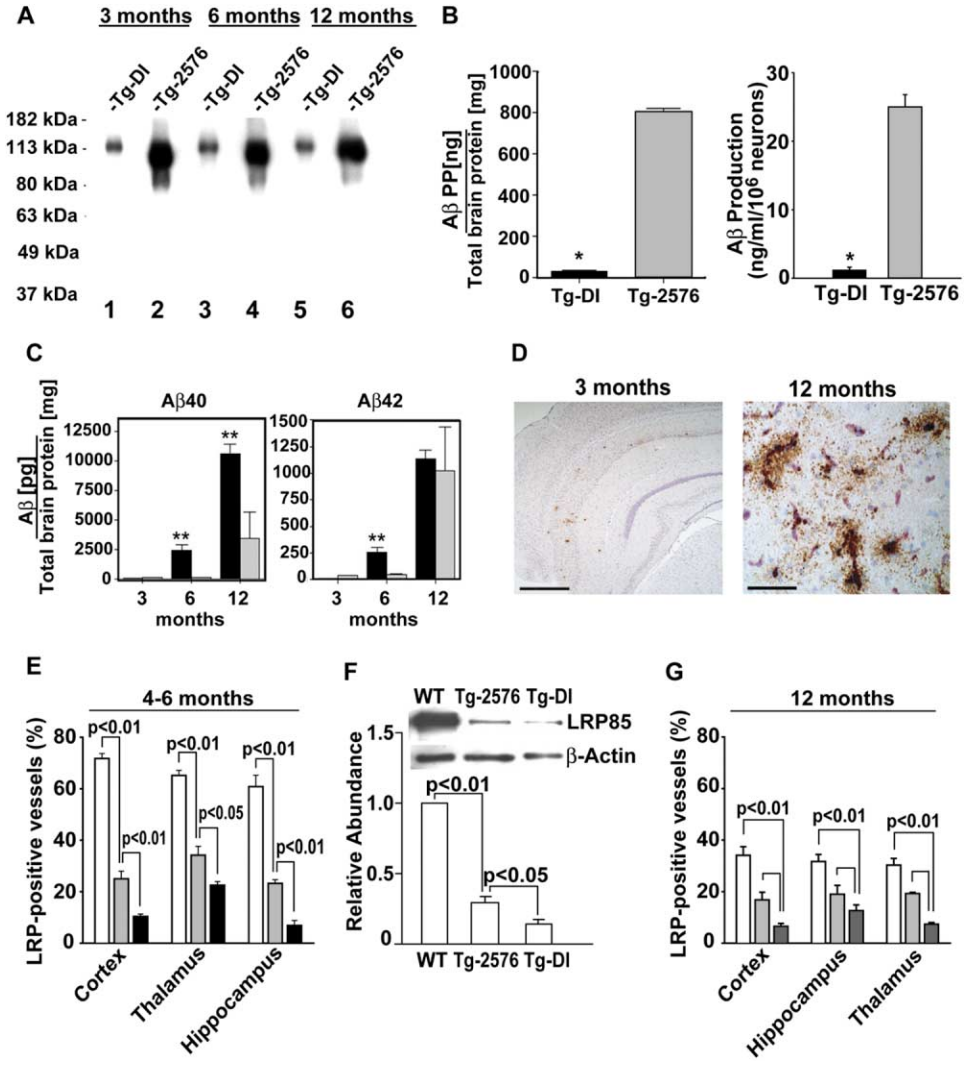

Figure 5. Aβ Accumulation in Transgenic Mice Expressing Low LRP-Clearance Mutant Aβ versus Wild-Type Aβ

(A) Immunoblot analysis of human APP in the brain of transgenic Tg-DI mice expressing mutant APP harboring Dutch and Iowa mutations versus Tg-2576 mice.

(B) APP levels in the brain of Tg-DI mice versus Tg-2576 mice at 6 months of age (left) and Aβ production from isolated mouse neurons into culture medium (right) determined by quantitative immunoblot analyses.

(C) Brain accumulation of low LRP-clearance mutant Aβ40 and Aβ42 (Dutch/Iowa, black bars) in Tg-DI mice versus wild-type Aβ40 and Aβ42 (gray bars) in Tg-2576 mice.

(D) Early deposits of mutant Aβ (Dutch/Iowa) in the brain of Tg-DI mice at 3 months of age (scale bar equals 200 μm), and abundant diffuse deposits with significant intracerebral microvascular Aβ deposits in Tg-DI mice at 12 months of age (scale bar equals 50 μm) detected by immunostaning for Aβ.

(E) LRP-positive brain microvessels in Tg-DI mice (black bars), Tg-2576 mice (gray bars), and controls (open bars) at 4–6 months of age.

(F) Western blot analysis of LRP levels in mice in (E).

(G) LRP-positive microvessels in Tg-DI mice (black bars), Tg-2576 mice (gray bars), and controls (open bars) at 12 months of age. Mean ± SEM (n = 4 mice). *$p < 0.001$ and **$p < 0.01$ in (B) and (C) for APP and Aβ levels in Tg-DI mice compared to Tg-2576 mice.

slow Aβ uptake into neurons isolated from transgenic APP mice (Qiu et al., 1999) as well as into mouse fibroblasts (Kang et al., 2000). Degradation of Aβ via α_2M in U97 human glioblastoma cells and mouse fibroblasts may also require LRP (Narita et al., 1997).

Despite extremely low human APP expression/Aβ production, i.e., 25- to 30-fold lower than Tg-2576 mice, Tg-DI mice (Davis et al., 2004) expressing low LRP-clearance mutant Aβ develop robust Aβ brain accumulations much earlier than Tg-2576 Aβ-overproducing mice (Figure 5; Hsiao et al., 1996; Kawarabayashi et al., 2001). Significant intraparenchymal microvascular Aβ association points to brain's blood vessels as a site of deficient clearance in Tg-DI mice consistent with prominent cerebrovascular pathology in Dutch and Iowa patients (Vinters and Farag, 2003). Increased fibrillogenicity of mutant Dutch/Iowa Aβ (Van Nostrand et al., 2001) may contribute to its decreased clearance from brain, but the presence of mainly nonfibrillar Aβ parenchymal deposits in Tg-DI mice would argue against this possibility.

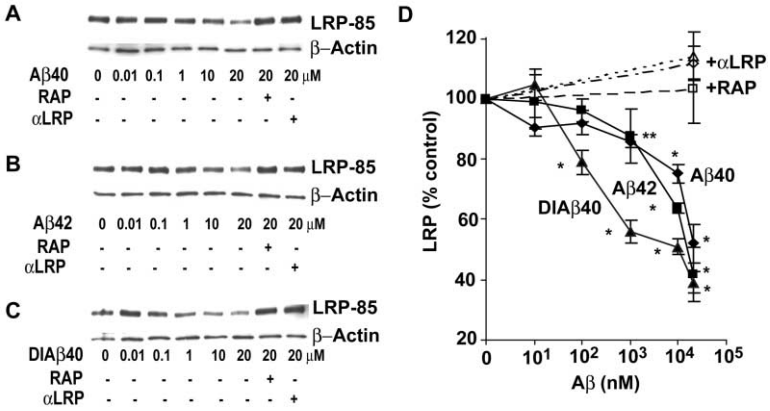

Figure 6. LRP Downregulation in Human Brain Endothelium by Excess Aβ

(A–C) Western blot analysis of LRP β subunit (LRP-85) in brain endothelium exposed for 48 hr to different concentrations of Aβ40, Aβ42, and mutant Aβ (Dutch/Iowa40; DIAβ40) from 1 nM to 20 μM. RAP (1.25 μM) and αLRP, LRP β-chain-specific IgG $F(ab)_2$ (25 μg/ml) were incubated 1 hr prior to the addition of Aβ peptides and then for 48 hr simultaneously with different Aβ peptides.

(D) Relative intensity of LRP bands in brain endothelium exposed to different Aβ peptides was determined by scanning densitometry and normalized for β-actin. Mean ± SEM (n = 3–5 independent experiments); *$p < 0.01$ and **$p < 0.05$ for the relative expression of LRP levels in the presence of a given Aβ concentration compared to the absence of Aβ.

In addition to reduced LRP-mediated Aβ efflux, an increased formation of nonfibrillar Aβ species might favor Aβ deposition in this model.

The present data show that Aβ at pathological concentrations reduces LRP levels in brain endothelium by accelerating proteasome-dependent LRP degradation (Melman et al., 2002), while the receptor's internalization and synthesis are not affected (Figures 6 and 7). In contrast to LRP downregulation by simultaneous overexpression of secreted ligands such as apoE, resulting in retention and degradation of LRP in the endoplasmic reticulum (ER) (Willnow et al., 1996; Herz and Marschang, 2003), binding of internalized Aβ to immature LRP in the ER compartment is not implicated in LRP degradation by extracellular Aβ. One can speculate that Aβ accumulations adjacent to brain vasculature may downregulate LRP at the BBB in vivo consistent with reduced brain capillary LRP levels in transgenic Aβ-accumulating mice (Figures 5E–5G), AD, and patients with the Dutch-type cerebrovascular β-amyloidosis (Figure 8) and reduced total brain LRP in AD (Kang et al., 2000; Shibata et al., 2000).

In contrast to LRP, RAGE mediates a continuous influx of circulating Aβ into the brain and is overexpressed in brain vasculature in transgenic APP models and in AD (Deane et al., 2003). Thus, an imbalance between LRP-mediated and RAGE-mediated Aβ transport at the BBB would create a positive feedback amplification mecha-

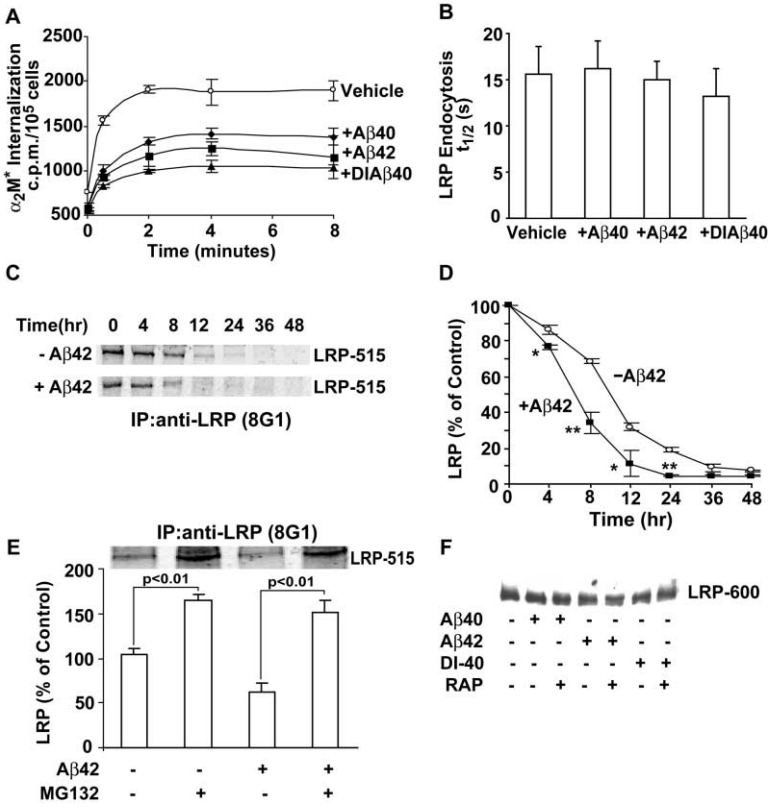

Figure 7. High Aβ Levels Reduce LRP's Half-Life in Human Brain Endothelium

(A) Internalization of [^{125}I]α2M* by human BEC treated with 20 μM of Aβ40, Aβ42, and mutant Aβ (DIAβ40) for 48 hr.

(B) The half-life ($t_{1/2}$) for rapid LRP endocytosis in human BEC in (A) determined with [^{125}I]α2M*.

(C) Cells were labeled by [^{35}S]methionine for 1 hr and chased for the indicated times. Autoradiograph of ^{35}S-methionine-labeled LRP immunoprecipitated with LRP 515 kDa α subunit-specific IgG in the presence and absence of Aβ42 (20 μM).

(D) Graph of LRP levels from three independent experiments as in (A). *$p < 0.05$ and **$p < 0.01$ in the presence of Aβ compared to the corresponding control value.

(E) Effects of the proteasomal inhibitor MG132 (20 μM) on LRP levels in the presence and absence of Aβ42 (20 μM) determined at 8 hr. Autoradiograph of ^{35}S-methionine-labeled LRP immunoprecipitated with LRP 515 kDa α subunit-specific IgG. Graph of LRP levels from three independent experiments as in (C).

(F) Western blot analysis for immature 600 kDa LRP (LRP-600) in the presence of Aβ40, Aβ42, or mutant Aβ (Dutch/Iowa40, DIAβ40) at 20 μM within 48 hr, as demonstrated with LRP-specific IgG directed to the C-terminal region of LRP (5A6). RAP was used at 1.2 μM. Mean ± SEM (n = 3) in (B) and (D).

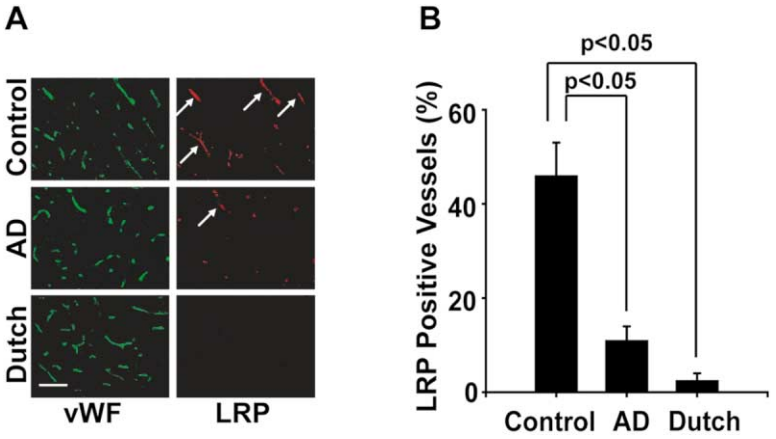

Figure 8. LRP Expression in Brain Microvessels in Alzheimer's and Dutch Patients

(A) Immunostaining for Von Willebrand factor (vWF, endothelial cell marker) and LRP in cortical sections (Brodman area 10) in age-matched controls and AD and Dutch patients with cerebrovasular β-amyloidosis. Scale bar equals 50 μm.

(B) LRP-positive vessels in controls, AD, and Dutch patients. Mean ± SEM (n = 4 cases/group).

nism for Aβ accumulation in AD and related familial cerebrovascular disorders. The present findings raise a possibility that efficacy of Aβ lowering therapies with peripheral Aβ sequestering agents (DeMattos et al., 2002a; Deane et al., 2003; Matsuoka et al., 2003) may depend at least in part on preserved LRP activity at the BBB. Whether therapeutic modifications of Aβ/LRP interaction at the BBB will have a major impact on controlling dementia remains to be seen in the future.

Experimental Procedures

Reagents

Wild-type and mutant Aβ (Dutch40, Dutch42, Dutch/Iowa40) peptides were synthesized by solid-phase F-moc (9-fluorenylmethoxycarbonyl) amino acid chemistry, purified by reverse phase-HPLC, and structurally characterized, as described (Burdick et al., 1992; Van Nostrand et al., 2001). Recombinant LRP fragments encompassing clusters II and IV were produced using stable transfected baby hamster kidney cell lines (Westein et al., 2002). We used human recombinant RAP (EMD Biosciences, Inc., San Diego, CA), polyclonal goat anti-human LRP N20 antibody, which crossreacts with mouse LRP (1:200, Santa Cruz Biotech. Inc., Santa Cruz, CA), monoclonal mouse antibody against C-terminal domain of human LRP β-chain, which crossreacts with mouse LRP (5A6, 1:350, 5 μg/ml; EMD), monoclonal mouse antibody against human LRP α chain (8G1,1:240, 5 μg/ml; EMD), monoclonal mouse antibody P2-1 specific for human APP (1:1000, 1 mg/ml), 22C11, which recognizes mouse and human APP (1:100, 0.5 mg/ml; Chemicon International, Temecula, CA), 66.1 to residues 1–8 of human Aβ (1:1000, 1 mg/ml) (Deane et al., 2003), rat anti-mouse CD31 antibody (1:200, BD Pharmigen, Lexington, KY), polyclonal rabbit antibody to human von Willebrand Factor, vWF (1:200, DAKO, Carpinteria, CA), RAGE-specific IgG (1:500, 1 mg/ml) (Deane et al., 2003), goat anti-human VLDLR (1:50, 200 μg/ml, Santa Cruz), and monoclonal mouse human LDLR-specific IgG C7 (1:50, 200 μg/ml, Research Diagnostics, Flanders, NJ).

Surface Plasmon Resonance Analysis

LRP clusters II and IV immobilized at CM5 chips at a density of 10–20 fmol/mm^2 and incubated with Aβ40, Aβ42, and mutant Aβ (Dutch/Iowa40) (0–50 nM) in 150 mM NaCl, 0.005% (v/v) Tween, and 25 mM HEPES (pH 7.4) at a flow rate of 5 μl/min for 2 min at 25°C, as described (Westein et al., 2002). RAP was used at 500 nM. The data were analyzed to calculate apparent association rate constant $k_{on(app)}$ and apparent dissociation rate constant $k_{off(app)}$ using a single-site binding model (Westein et al., 2002). Apparent affinity constant $K_{d(app)}$ was inferred from the ratio $k_{off(app)}/k_{on(app)}$. Data are based on 3–5 measurements using 6–9 different concentrations for each measurement and presented as the average (±SEM). Analysis was performed using Biacore X biosensor system (Uppsala, Sweden) and BIA evaluation 3.0 software (Biocore, Sweden).

Secondary Structure Analysis

Secondary structure of peptides was analyzed by circular dichroism (Zlokovic et al., 1996; Golabek et al., 1996). Briefly, 20–25 μg of hexafluoroisopropanol-treated seedless peptide was dissolved in 980 μl of 10 mM phosphate buffer (pH 7.4) and centrifuged to remove precipitated/undissolved material. The CD spectrum was recorded within 24 hr using a 1 mm path length cell on an Aviv 202 CD spectropolarimeter (Proterion, Piscataway, NJ). Results are expressed as molar ellipticity and the percentage of α helix, β sheet, β-turn, and random coil determined.

Radioiodination of Aβ

Radioiodination of Aβ was carried out by mild "lactoperoxidase" method (Thorell and Johansson, 1971). Typically, 10 μg of Aβ was labeled for 18 min at room temperature with 2 mCi of [^{125}I]Na. After radiolabeling, the preparations were subjected to reverse-phase HPLC separation using a Vydac C4 column and a 30 min linear gradient of 25% to 40% acetonitrile in 0.059% trifluoroacetic acid to separate the monoiodinated nonoxidized form of Aβ (which is the tracer we are using) from diiodinated Aβ, nonlabeled nonoxidized Aβ, and oxidized Aβ species, as we reported (Deane et al., 2003). The content of material in the peaks eluted from HPLC was determined by MALDI-TOF mass spectrometry to ensure the purity of the radiolabeled species. For MALDI-TOF mass spectrometry, Aβ peptides were labeled under identical conditions using [^{127}I]Na instead of the radioactive nuclide. The specific activities were in the range of 45 to 65 μCi/μg of peptide. For brain capillary uptake studies and animal clearance studies, we used in most experiments the preparations within 24 hr of labeling that were ≥99% TCA-precipitable. If used within 72 hr of labeling, the radiolabeled peptides were stabilized in ethanol as a quenching agent. The HPLC/SDS-PAGE analysis was used to confirm the monomeric state of infused radiolabeled Aβ.

Brain Capillary Binding, Endocytosis, and Uptake of [^{125}I]Aβ

Brain capillaries from wild-type, RAP null, LDLR null, and VLDLR null mice were isolated using a modified procedure, as we described (Wu et al., 2003).

First, we determined ^{125}I-labeled Aβ40, Aβ42, Dutch/Iowa Aβ40, and reverse 40-1 Aβ binding to endogenous LRP at the abluminal side of brain capillaries. Capillaries were incubated in 0.6 ml Eppendorf tubes in the assay buffer (mock CSF containing 1 mM sodium perchlorate to prevent free iodide binding/uptake) with 2 nM [^{125}I]Aβ ligand at 4°C for 30 min in the absence and presence of RAP (500 nM), LRP-specific IgG (Fab_2), and unlabeled Aβ (500 nM). After 30 min, incubation buffer containing unbound ligand was removed and capillaries washed, lysed in low SDS lysis buffer, and counted.

Second, we determined internalization of ^{125}I-labeled Aβ40, Aβ42, and Dutch/Iowa Aβ40 at the abluminal surface of brain capillaries and the rate of LRP endocytosis in the presence of each isoform. Capillaries were incubated in 0.6 ml Eppendorf tubes in cold assay buffer with 2 nM [^{125}I]Aβ ligand at 4°C for 30 min in the absence and presence of RAP (500 nM), LRP-specific IgG (Fab_2), and unlabeled

Aβ (500 nM), as above. After 30 min, unbound ligand was removed by washing capillaries with cold assay buffer. Ice-cold stop/strip solution (0.2 M acetic acid [pH 2.6], 0.1 M NaCl) was added to one Eppendorf tube that was kept on ice. The remaining Eppendorf tubes were placed in a 37°C water bath, and the assay buffer at 37°C was added quickly to capillaries to initiate ligand internalization. At predetermined times at 30 s and 1, 2, and 5 min, Eppendorf tubes were quickly placed on ice and incubated for 12 min with the ice-cold stop/strip solution (0.2 M acetic acid [pH 2.6], 0.1 M NaCl) to remove ligand from the capillary abluminal cell surface. Capillaries were solubilized with low SDS lysis buffer and counted. The sum of internalized ligand plus the ligand associated with the abluminal capillary cell surface represented the amount of ligand available for internalization. The fraction of ligand internalized at each time point was plotted, and the half-time for internalization ($t_{1/2}$) was calculated, as described (Li et al., 2001).

[^{125}I]Aβ ligand degradation was determined in brain capillary endothelial cell lysates and in the incubation medium at the end of internalization studies using the TCA precipitation assay, as reported (Deane et al., 2003).

To determine kinetics of [^{125}I]Aβ brain capillary unidirectional uptake, capillaries were incubated with ^{125}I-labeled Aβ40, Aβ42, and mutant Aβ (Dutch/Iowa40) at 37°C for 1 min. Self- and crossinhibition studies were performed with unlabeled Aβ40 from 1 to 120 nM and unlabeled Aβ42 and mutant Aβ (Dutch40, Dutch42, Dutch/Iowa40) at 40 nM, RAP (500 nM), and LRP-specific polyclonal N20 antibody (60 μg/ml).

Brain Clearance Studies

Studies were performed according to the National Institutes of Health guidelines using an approved institutional protocol. CNS clearance of ^{125}I-labeled Aβ ligands was determined simultaneously with [^{14}C]inulin (reference marker) in male C57Bl/6, RAP null, LDLR null, and VLDLR null mice 8–10 weeks old, using a procedure as described (Shibata et al., 2000). Briefly, a stainless steel guide cannula was implanted stereotaxically into the right caudate-putamen of anesthetized mice (0.5 mg/kg ketamine and 5 mg/kg xylazine i.p.). Coordinates for tip of the cannula were 0.9 mm anterior and 1.9 mm lateral to the bregma and 2.9 mm below the surface of the brain. Animals were allowed to recover after surgery prior to radiotracer studies. The experiments were performed before substantial chronic processes occurred, as assessed by histological analysis of tissue, i.e., negative staining for astrocytes (glial fibrillar acidic protein) and activated microglia (anti-phosphotyrosine), but allowing time for BBB repair to large molecules (Zlokovic et al., 2000), typically 4–6 hr after the cannula insertion, as reported (Cirrito et al., 2003). Tracer fluid (0.5 μl) containing [^{125}I]Aβ and [^{14}C]inulin was injected into brain ISF over 5 min via an ultra micropump with a micro4-controller (World Precision Instruments, Sarasota, FL). When the effects of different unlabeled molecular reagents are tested, these were injected simultaneously with radiolabled ligands. For self-inhibition studies, the uptake of ^{125}I-labeled Aβ40 and mutant Aβ (Dutch/Iowa40) was studied over a range of carrier concentrations from 0.5 to 120 nM. For crossinhibition studies, efflux of ^{125}I-labled test peptides was studied at a carrier concentration of 40 nM and the inhibitory concentration of unlabeled Aβ peptides at 120 nM. Brain and blood were sampled 30 min after tracer injection and prepared for radioactivity analysis by TCA, HPLC, and SDS-PAGE/immunoprecipitation analysis to determine the molecular forms of test tracers, as described (Zlokovic et al., 1996; Shibata et al., 2000; Deane et al., 2003). Gamma counting was performed using Wallac Vizard Gamma Counter (Perkin Elmer, Meriden, CT) and β-counting using Tri-carb 2100 Liquid Scintillation Counter (Perkin Elmer, CT). Previous studies with ^{125}I-labeled Aβ demonstrated an excellent correlation between TCA and HPLC methods. The intactness of ^{125}I-labeled Aβ40, Aβ42, and mutant Aβ (Dutch/Iowa40) injected into the brain ISF was >99% by TCA/HPLC analysis. The Aβ standards eluted between 29.1 and 31.2 min for different Aβ peptides. For SDS-PAGE analysis, TCA-precipitated samples were resuspended in 1% SDS, vortexed, and incubated at 55°C for 5 min, then neutralized, boiled for 3 min, homogenized, and analyzed by electrophoresis in 10% Tris-tricine gels followed by fluorography. Methodological details were as we reported (Zlokovic et al., 1996; Shibata et al., 2000; Deane et al., 2003).

Calculations

[^{125}I]Aβ brain capillary uptake was corrected for the distribution of [^{14}C]inulin (extracellular space marker) and determined as the tissue to medium ratio: c.p.m. for TCA-precipitable ^{125}I-radioactivity (mg capillary protein)/c.p.m. for TCA-precipitable ^{125}I-radioactivity (ml medium). All calculations of clearance parameters were as reported (Shibata et al., 2000). Briefly, the percentage of radioactivity remaining in the brain after microinjection was determined as % recovery in brain $= 100 \times (N_b/N_i)$, where N_b is the radioactivity remaining in the brain at the end of the experiment and N_i is the radioactivity injected into the brain ISF, i.e., the d.p.m. for [^{14}C]inulin and the c.p.m. for TCA-precipitable [^{125}I]radioactivity (intact Aβ). The percentage of Aβ cleared through the BBB was calculated as $[(1 - N_{b(A\beta)}/N_{i(A\beta)}) - (1 - N_{b(inulin)}/N_{i(inulin)})] \times 100$, using a standard time of 30 min. Efflux of Aβ from brain ISF via transport across the BBB at different concentrations of peptides, J_{out}, was calculated as $[(1 - N_{b(A\beta)}/N_{i(A\beta)}) - (1 - N_{b(inulin)}/N_{i(inulin)})]/T \times C_{A\beta}$, where $C_{A\beta}$ is Aβ concentration in the infusate. The half-saturation concentration for Aβ elimination via BBB transport, K_m, was calculated from $J_{out} = Cl_{max}/(K_m + C_{A\beta})$, where Cl_{max} (pmol/s/l ISF) represents the maximal efflux capacity for the saturable Aβ efflux across the BBB corrected for the rate of ISF flow, as we reported (Shibata et al., 2000). The K_m value for Aβ40 uptake by isolated brain capillaries was calculated using Michaelis-Menten analysis. The inhibitory constants, K_i, were calculated from the velocity ratios (Zlokovic et al., 1996) as $K_i = (J_i \times K_m \times C_i)/(J_{out} - J_i)(K_m + C_{A\beta40})$, where C_i and $C_{A\beta40}$ were the inhibitory concentrations of test Aβ peptide and Aβ40 in the infusate in vivo or incubation medium in vitro. Kinetic constants were obtained by a nonlinear regression curve fitting (Prism 3.0).

Transgenic Mice

We used Tg-2576 mice in a C57Bl6/SJL background (Hsiao et al., 1996) and Tg-DI (Dutch/Iowa) mice in C57Bl6 background (Davis et al., 2004). Human APP (770 isoform) cDNA harboring the Swedish (KM670/671NL), Dutch (E693Q), and Iowa (D694N) mutations was subcloned between exons II and IV of a Thy-1.2 expression cassette (gift from Dr. F. LaFerla, UC Irvine, Irvine, CA). The 9 kb transgene was liberated by NotI/PvuI digestion, purified, and microinjected into pronuclei of C57BL/6 single cell embryos at the Stony Brook Transgenic Mouse Facility. Founder transgenic mice were identified by Southern blot analysis of tail DNA. Transgenic offspring were determined by PCR analysis of tail DNA using the following primers for human APP: 5′-CCTGATTGATACCAAGGAAGGCATCCTG-3′:5′-GTCATCATCGGCTTCTTCTTCTTCCACC-3′ (generating 500 base pair product). RAP null, VLDLR null, and LDLR null mice were purchased from Jackson Laboratories (Bar Harbor, ME).

Quantification of Aβ

Soluble and insoluble pools of Aβ were determined by ELISA of carbonate extracted forebrain tissue and of guanidine lysates of the insoluble pellets resulting from the carbonate extracted brain tissue, respectively (DeMattos et al., 2002b). Levels of total Aβ were compared between Tg-2576 and Tg-DI mice.

Histological Analysis

For neuropathological analysis on mouse brain tissue in Tg-2576 and Tg-DI mice, tissue sections were cut from mouse brain hemispheres in the sagittal plane either at 5 μm (paraffin embedded fixed tissue) or 14 μm (fresh frozen tissue). Aβ immunoreactive deposits were identified with human-specific monoclonal mouse antibody 66.1 to Aβ (Deane et al., 2003). For LRP staining on brain microvessels in RAP null, Tg-2576, Tg-DI, and wild-type mice, we used 14 μm frozen acetone fixed tissue sections and double imunostaining for LRP and CD31 (endothelial marker). LRP-specific IgG (5A6) was used as a primary antibody. Biotinylated anti-mouse IgG was used as a secondary antibody and was detected with fluorescein streptavidin (1:1000, Vector Laboratories, Inc., Burlingame, CA). M.O.M kit (Vector) was used to block endogenous IgG, as described (Sata et al., 2002). For CD31 staining, mouse CD31-specific IgG was used as a primary antibody and Alexa Fluor 594 donkey anti-rat IgG (1:500, Molecular Probes, Eugene, OR) as a secondary antibody. For immunocytochemical analysis of LRP on brain microvessels in tissue from AD patients, patients with cerebrovascular β-amyloidosis Dutch-

type, and age-matched controls, we used cryostat sections (10 μm) of frontal cortex (Brodmann area 9/10) that were air dried. LRP was detected with 8G1 human LRP-specific IgG as a primary antibody and rhodamine red goat anti-mouse IgG (1:150, Molecular Probes) as a secondary antibody. The anti-vWF (endothelial marker) primary antibody was detected with fluorescein goat anti-rabbit IgG (1:150, Molecular Probes). Image analysis was performed using Olympus AX70 microscope equipped with the SPOT digital camera. Ten randomly selected fields in each region from ten sections spanning the entire hemisphere from 4 mice/group or from Brodman A9/10 areas in humans was performed.

Human Brain Endothelial Cells

Human BEC were isolated from rapid autopsies of neurologically normal young individuals after trauma. BECs were characterized and cultured as we described (Cheng et al., 2003) and incubated with different Aβ isoforms at concentrations ranging from 1 nM to 20 μM within 48 hr. Cells were lysed and equal amounts of proteins electrophoresed (10 μg/ml) on 10% SDS-polyacrillamide gel, transferred onto nitrocellulose membrane, and probed with 5A6 (β-chain) or 8G1 (α chain) human LRP-specific IgGs, RAGE-specific IgG (Deane et al., 2003), or transferrin-specific IgG. The relative density of each protein was determined by scanning densitometry using β-actin as an internal control.

LRP endocytosis rates were studied with [^{125}I]α2M*, an LRP-specific ligand. BEC were incubated with 20 μM Aβ40, Aβ42, and Dutch/Iowa Aβ40 at 37°C for 48 hr in 12-well plates and then switched to Aβ-free medium containing 5 mM $CaCl_2$ and 5 nM [^{125}I]α2M* at 4°C for 30 min followed by incubations with α2M*-free medium at 37°C to initiate internalization, as reported (Li et al., 2001).

Metabolic Labeling

Human BEC (4×10^5) were pulsed for 1 hr at 37°C with 400 μCi of [^{35}S]methionine (>1000 Ci/mmol; Perkin Elmer Life Sci. Inc., Boston, MA) in methionine-free Dulbecco modified Eagle medium (GIBCO-BRL, New York, NY), as described (Guenétte et al., 2002). Cells were chased at indicated times within 48 hr. Cell lysates were immunoprecipitated with LRP-515 kDa α chain specific IgG (8G1) on SDS-PAGE. The intensity of signal was quantified in pixels using Storm 860 Phosphoimager (Amersham Biosciences Corp., Piscataway, NJ).

Neuronal Cultures and Aβ Production

Primary mouse neuronal cultures were prepared as we described (Guo et al., 2004). Briefly, cerebral cortices were dissected from fetal heterozygous Tg-DI mice (Davis et al., 2004) and Tg-2576 mice (Hsiao et al., 1996) at 16 days of gestation, treated with trypsin for 10 min at 37°C, and dissociated with trituration. Cell suspensions were plated at 5×10^5 cells per well on 12-well plates in serum-free Neurobasal medium plus B27 supplement (GIBCO-BRL, Rockville, MA). The absence of astrocytes was confirmed by the lack of glial fibrillar acidic protein. Cultures were maintained in a humidified 5% CO_2 incubator at 37°C for 5 days and the levels of Aβ in the culture medium determined by a quantitative immunoblot analysis using 4G8 antibody (1:1000, 1 μg/ml, Signet, Dedham, MA), similar as described (Qiu et al., 1999).

Statistical Analysis

Data were analyzed by multifactorial analysis of variance, Student's t test, and Dunnett's t test.

Acknowledgments

This research was supported by grants AG16223, NS34467, and AG23084 from the US Public Health Service to B.V.Z. and NS36645 to W.E.V.N. We thank Dr G. Bu for the initial supply of RAP. The authors of this paper have declared a conflict of interest. For details, go to http://www.neuron.org/cgi/content/full/43/3/333/DC1.

Received: February 9, 2004
Revised: April 23, 2004
Accepted: July 14, 2004
Published: August 4, 2004

References

Bu, G. (2001). The roles of receptor-associated protein (RAP) as a molecular chaperone for members of the LDL receptor family. Int. Rev. Cytol. *209*, 79–116.

Burdick, D., Soreghan, B., Kwon, M., Kosmoski, J., Knauer, M., Henscehn, A., Yates, J., Cotman, C., and Glabe, C. (1992). Assembly and aggregation properties of synthetic Alzheimer's A4/β amyloid peptide analogs. J. Biol. Chem. *267*, 546–554.

Cheng, T., Liu, D., Griffin, J.H., Fernandez, J.A., Castellino, F., Rosen, E.D., Fukudome, K., and Zlokovic, B.V. (2003). Activated protein C blocks p53-mediated apoptosis in ischemic human brain endothelium and is neuroprotective. Nat. Med. *9*, 338–342.

Cirrito, J.R., May, P.C., O'Dell, M.A., Taylor, J.W., Parsadanian, M., Cramer, J.W., Audia, J.E., Nissen, J.S., Bales, K.R., Paul, S.M., et al. (2003). In vivo assessment of brain interstitial fluid with microdialysis reveals plaque-associated changes in amyloid-β metabolism and half-life. J. Neurosci. *23*, 8844–53.

Dahlgren, K.N., Manelli, A.M., Stine, W.B., Baker, L.K., Krafft, G.A., and LaDu, M.J. (2002). Oligomeric and fibrillar species of amyloid-β peptides differentially affect neuronal viability. J. Biol. Chem. *277*, 32046–32053.

Davis, J., Xu, F., Deane, R., Romanov, G., Prevetti, M.L., Zeigler, K., Zlokovic, B.V., and Van Nostrand, W. (2004). Early-onset and robust cerebral microvascular accumulation of amyloid β-protein in transgenic mice expressing low levels of a vasculotropic Dutch/Iowa mutant form of amyloid β-protein precursor. J. Biol. Chem. *279*, 20296–20306.

Deane, R., Du Yan, S., Submamaryan, R.K., LaRue, B., Jovanovic, S., Hogg, E., Welch, D., Manness, L., Lin, C., Yu, J., et al. (2003). RAGE mediates amyloid-β transport across the blood-brain barrier and accumulation in brain. Nat. Med. *9*, 907–913.

DeMattos, R.B., Bales, K.R., Cummins, D.J., Paul, S.M., and Holtzman, D.M. (2002a). Brain to plasma amyloid-Aβ efflux: a measure of brain amyloid burden in a mouse model of Alzheimer's disease. Science *295*, 2264–2267.

DeMattos, R.B., O'Dell, M.A., Parsadanian, M., Taylor, J.W., Harmony, J.A., Bales, K.R., Paul, S.M., Aronow, B.J., and Holtzman, D.M. (2002b). Clusterin promotes amyloid plaque formation and is critical for neuritic toxicity in a mouse model of Alzheimer's disease. Proc. Natl. Acad. Sci. USA *99*, 10843–10849.

Flood, D.G., Reaume, A.G., Dorfman, K.S., Lin, Y.-G., Lang, D.M., Trusko, S.P., Savage, M.J., Annaert, W.G., De Strooper, B., Siman, R., and Scott, R.W. (2002). FAD mutant PS-1 gene-targeted mice: increased Aβ42 and Aβ deposition without APP overproduction. Neurobiol. Aging *23*, 335–348.

Ghiso, J., and Francione, B. (2002). Amyloidosis and Alzheimer's disease. Adv. Drug Deliv. Rev. *54*, 1539–1551.

Golabek, A.A., Soto, C., Vogel, T., and Wisniewski, T. (1996). The interaction between apolipoprotein E and Alzheimer's amyloid beta-peptide is dependent on beta-peptide conformation. J. Biol. Chem. *271*, 10602–10606.

Grabowski, T.J., Cho, H.S., Vonsattel, J.P.G., Rebeck, G.W., and Greenberg, S.M. (2001). Novel amyloid precursor protein mutation in an Iowa family with dementia and severe cerebral amyloid angiopathy. Ann. Neurol. *49*, 697–705.

Gong, Y., Chang, L., Viola, K.L., Lacor, P.N., Lambert, M.P., Finch, C.E., and Krafft, G.A. (2003). Alzheimer's disease-affected brain: presence of oligomeric Aβ ligands (ADDLs) suggests a molecular basis for reversible memory loss. Proc. Natl. Acad. Sci. USA *100*, 10417–10422.

Green, P., and Bu, G. (2002). Genetics and molecular biology: phosphorylation of low-density lipoprotein receptor-related proein by platelet-derived growth factor. Curr. Opin. Lipidol. *13*, 569–572.

Guenétte, S.Y., Ghang, Y., Hyman, B.T., Tanzi, R.E., and Rebeck, G.W. (2002). Low-density lipoprotein receptor-related protein levels and endocytic function are reduced by overexpression of the FE65 adaptor protein, FE65L1. J. Neurochem. *82*, 755–762.

Guo, H., Liu, D., Gelbard, H., Cheng, T., Fernandez, J.A., Insalaca, R., Griffin, J.H., and Zlokovic, B.V. (2004). Activated protein C prevents

neuronal apoptosis via protease activated receptors 1 and 3. Neuron *41*, 563–572.

Hardy, J., and Selkoe, D.J. (2002). The amyloid hypothesis of Alzheimer's disease: progress and problems on the road to therapeutics. Science *297*, 353–356.

Herz, J. (2001). The LDL receptor gene family: (un)expected signal transducers in the brain. Neuron *29*, 571–581.

Herz, J., and Strickland, D.K. (2001). LRP: a multifunctional scavenger and signaling receptor. J. Clin. Invest. *108*, 779–784.

Herz, J., and Marschang, P. (2003). Coaxing the LDL receptor family into the blood. Cell *112*, 289–292.

Herz, J., Kowal, R.C., Goldstein, J.L., and Brown, M.S. (1990). Proteolytic processing of the 600 kd low density lipoprotein receptor-related protein (LRP) occurs in a trans-Golgi compartment. EMBO J. *9*, 1769–1776.

Hollenbach, E., Ackermann, S., Hyman, B.T., and Rebeck, G.W. (1998). Confirmation of an association between a polymorphism in exon 3 of the low-density lipoprotein receptor-related protein gene and Alzheimer's disease. Neurology *50*, 1905–1907.

Hsiao, K., Chapman, P., Nilsen, S., Eckman, C., Harigaya, Y., Younkin, S., Yang, F., and Cole, G. (1996). Correlative memory deficits, Aβ elevation, and amyloid plaques in transgenic mice. Science *274*, 99–102.

Jordán, J., Galindo, M.F., Miller, R.J., Reardon, C.A., and Getz, G.S. (1998). Isoform-specific effect of apolipoprotein E on cell survival and β-amyloid-induced toxicity in rat hippocampal pyramidal neuronal cultures. J. Neurosci. *18*, 195–204.

Kang, D.E., Saitoh, T., Chen, X., Xia, Y., Masliah, E., Hansen, L.A., Thomas, R.G., Thal, L.J., and Katzman, R. (1997). Genetic association of the low-density lipoprotein receptor-related protein gene (LRP), an apolipoprotein E receptor, with late-onset Alzheimer's disease. Neurology *49*, 56–61.

Kang, D.E., Pietrzik, C.U., Baum, L., Chevallier, N., Merriam, D.E., Kounnas, M.Z., Wagner, S.L., Troncoso, J.C., Kawas, C.H., Katzman, R., and Koo, E.H. (2000). Modulation of amyloid β-protein clearance and Alzheimer's disease susceptibility by the LDL receptor-related protein pathway. J. Clin. Invest. *106*, 1159–1166.

Kawarabayashi, T., Younkin, L.H., Saido, T.C., Shoji, M., Ashe, K.H., and Younkin, S.G. (2001). Age-dependent changes in brain, CSF, and plasma amyloid Aβ protein in the Tg2576 transgenic mouse model of Alzheimer's disease. J. Neurosci. *21*, 372–381.

Kayed, R., Head, E., Thompson, J.L., McIntire, T.M., Milton, S.C., Cotman, C.W., and Glabe, C.G. (2003). Common structure of soluble amyloid oligomers implies common mechanism of pathogenesis. Science *300*, 486–489.

Kounnas, M.Z., Moir, R.D., Rebeck, G.W., Bush, A.I., Argraves, W.S., Tanzi, R.E., Hymann, B.T., and Strickland, D.K. (1995). LDL receptor-related protein, a multifunctional ApoE receptor, binds secreted beta-amyloid precursor protein and mediates its degradation. Cell *82*, 331–340.

Lambert, J.C., Wavrant-De Vrieze, F., Amouyel, P., and Chartier-Harlin, M.C. (1998). Association at LRP gene locus with sporadic late-onset Alzheimer's disease. Lancet *351*, 1787–1788.

Levy, E., Carman, M.D., Fernandez-Madrid, I.J., Power, M.D., Lieberberg, I., van Duinen, S.G., Bots, G.T., Luyendijk, W., and Frangione, B. (1990). Mutation of the Alzheimer's disease amyloid gene in hereditary cerebral hemorrhage, Dutch type. Science *248*, 1124–1126.

Li, Y., Lu, W., Marzolo, M.P., and Bu, G. (2001). Differential functions of members of the low density lipoprotein receptor family suggested by their distinct endoytosis rates. J. Biol. Chem. *276*, 18000–18006.

Mackic, J.B., Stins, M., McComb, J.G., Calero, M., Ghiso, J., Kim, K.S., Yan, S.D., Stern, D., Schmidt, A.M., Frangione, B., and Zlokovic, B.V. (1998). Human blood-brain barrier receptors for Alzheimer's amyloid-β 1–40: asymmetrical binding, endocytosis and transcytosis at the apical side of brain microvascular endothelial cell monolayer. J. Clin. Invest. *102*, 734–743.

Matsuoka, Y., Saito, M., LaFrancois, J., Saito, M., Taylor, K., Olm, V., Wang, L., Casey, E., Lu, Y., Shiratori, C., et al. (2003). Novel therapeutic approach for the treatment of Alzheimer's disease by peripheral administration of agents with an affinity to Aβ-amyloid. J. Neurosci. *23*, 29–33.

Melman, L., Geuze, H.J., Li, Y., McCormick, L.M., van Kerkhof, P., Strous, G.J., Schwartz, A.L., and Bu, G. (2002). Proteasome regulates the delivery of LDL receptor-related protein into the degradation pathway. Mol. Biol. Cell *13*, 3325–3335.

Narita, M., Holtzman, D.M., Schwartz, A.L., and Bu, G. (1997). α_2-macroglobulin complexes with and mediates the endocytosis of β-amyloid peptide via cell surface low-density lipoprotein receptor-related protein. J. Neurochem. *69*, 1904–1911.

Pietrzik, C.U., Busse, T., Merriam, D.E., Weggen, S., and Koo, E.H. (2002). The cytoplasmic domain of the LDL receptor-related protein regulates multiple steps in APP processing. EMBO J. *21*, 5691–5700.

Qiu, Z., Strickland, D.K., Hyman, B.T., and Rebeck, G.W. (1999). α_2-macroglobulin enhances the clearance of endogenous soluble β-amyloid peptide via low-density lipoprotein receptor-related protein in cortical neurons. J. Neurochem. *73*, 1393–1398.

Sata, M., Saiura, A., Kunisato, A., Tojo, A., Okada, S., Tokuhisa, T., Hirai, H., Makuuchi, M., Hirata, Y., and Nagai, R. (2002). Hematopoietic stem cells differentiate into vascular cells that participate in the pathogenesis of atherosclerosis. Nat. Med. *8*, 403–409.

Selkoe, D.J. (2001). Clearing the brain's amyloid cobwebs. Neuron *32*, 177–180.

Shibata, M., Yamada, S., Kumar, S.R., Calero, M., Bading, J., Frangione, B., Holtzman, D.M., Miller, C.A., Strickland, D.K., Ghiso, J., and Zlokovic, B.V. (2000). Clearance of Alzheimer's amyloid-$A\beta_{1-40}$ peptide from brain by low-density lipoprotein receptor-related protein-1 at the blood-brain barrier. J. Clin. Invest. *106*, 1489–1499.

Thorell, J.I., and Johansson, B.G. (1971). Enzymatic iodination of polypeptides with ^{125}I to high specific activity. Biochim. Biophys. Acta *251*, 363–366.

Ulery, P.G., Beers, J., Mikhailenko, I., Tanzi, R.E., Rebeck, G.W., Hyman, B.T., and Strickland, D.K. (2000). Modulation of β-amyloid precursor protein processing by the low density lipoprotein receptor-related protein (LRP). Evidence that LRP contributes to the pathogenesis of Alzheimer's disease. J. Biol. Chem. *275*, 7410–7415.

van der Geer, P. (2002). Phosphorylation of LRP1: regulation of transport and signal transduction. Trends Cardiovasc. Med. *12*, 160–165.

Van Nostrand, W.E., Melchor, J.P., Cho, H.S., Greenberg, S.M., and Rebeck, G.W. (2001). Pathogenic effects of D23N "Iowa" amyloid β-protein. J. Biol. Chem. *276*, 32860–32866.

Van Uden, E., Mallory, M., Veinbergs, I., Alford, M., Rockenstein, E., and Masliah, E. (2002). Increased extracellular amyloid deposition and neurodegeneration in human amyloid precursor protein transgenic mice deficient in receptor-associated protein. J. Neurosci. *22*, 9298–9304.

Veinbergs, I., Van Uden, E., Mallory, M., Alford, M., McGiffert, C., DeTeresa, R., Orlando, R., and Masliah, E. (2001). Role of apolipoprotein E receptors in regulating the differential in vivo neurotrophic effects of apolipoprotein E. Exp. Neurol. *170*, 15–26.

Vinters, H.V., and Farag, E.S. (2003). Amyloidosis of cerebral arteries. Adv. Neurol. *92*, 105–112.

Walsh, D.M., Klyubin, I., Fadeeva, J.V., Cullen, W.K., Anwyl, R., Wolfe, M.S., Rowan, M.J., and Selkoe, D.J. (2002). Naturally secreted oligomers of amyloid β protein potently inhibit hippocampal long-term potentiation in vivo. Nature *416*, 535–539.

Wang, X., Lee, S., Arai, K., Lee, S., Tsuji, K., Rebeck, G.W., and Lo, E.H. (2003). Lipoprotein receptor-mediated induction of matrix metalloproteinase by tissue plasminogen activator. Nat. Med. *9*, 1313–1317.

Wavrant-DeVrieze, F., Lambert, J.C., Stas, L., Crook, R., Cottel, D., Pasquier, F., Frigard, B., Lambrechts, M., Thiry, E., Amouyel, P., et al. (1999). Association between coding variability in the LRP gene and the risk of late-onset Alzheimer's disease. Hum. Genet. *104*, 432–434.

Westein, E., Denis, C.V., Bouma, B.N., and Lenting, P.J. (2002). The α-chains of C4b-binding protein mediate complex formation with

low density liporpoprotein receptor-related protein. J. Biol. Chem. *277*, 2511–2516.

Willnow, T.E., Rohlmann, A., Horton, J., Otani, H., Braun, J.R., Hammer, R.E., and Herz, J. (1996). RAP, a specialized chaperone, prevents ligand-induced ER retention and degradation of LDL receptor-related endocytic receptors. EMBO J. *15*, 2632–2639.

Wu, Z., Hofman, F.M., and Zlokovic, B.V. (2003). A simple method for isolation and characterization of mouse brain microvascular endothelial cells. J. Neurosci. Methods *130*, 53–63.

Zerbinatti, C.V., Wozniak, D.F., Cirrito, J., Cam, J.A., Osaka, H., Bales, K.R., Zhuo, M., Paul, S.M., Holtzman, D.H., and Bu, G. (2004). Increased soluble amyloid β peptide and memory deficits in amyloid model mice overexpressing the LDL receptor-related protein. Proc. Natl. Acad. Sci. USA *101*, 1075–1080.

Zlokovic, B.V., and Frangione, B. (2003). Transport-clearance hypothesis for Alzheimer's disease and potential therapeutic implications. In Aβ Metabolism in Alzheimer's Disease, T. Saido, ed. (Georgetown, TX: Landes Bioscience), pp. 114–122.

Zlokovic, B.V., Martel, C.L., Matsubara, E., McComb, J.G., Zheng, G., McCluskey, R.T., Frangione, B., and Ghiso, J. (1996). Glycoprotein 330/megalin: probable role in receptor-mediated transport of apolipoprotein J alone and in a complex with Alzheimer's disease amyloid-Aβ at the blood-brain and blood-cerebrospinal fluid barriers. Proc. Natl. Acad. Sci. USA *93*, 4229–4236.

Zlokovic, B.V., Yamada, S., Holtzman, D., Ghiso, J., and Frangione, B. (2000). Clearance of amyloid-Aβ-peptide from brain: transport or metabolism? Nat. Med. *6*, 718–719.